Conf-950201--11

UCRL-JC- 119681
PREPRINT

CREEP OF A FINE-GRAINED, FULLY-LAMELLAR, TWO-PHASE TiAl ALLOY AT 760°C

J. N. Wang
A. J. Schwartz
T. G. Nieh
C. T. Liu
V. K. Sikka
D. Clemens

This paper was prepared for submittal to
124th TMS Annual Meeting
in Las Vegas, NV on February 12-16, 1995.

February 1995

Lawrence Livermore National Laboratory

DISCLAIMER

CREEP OF A FINE-GRAINED, FULLY-LAMELLAR, TWO-PHASE TiAl ALLOY AT 760°C

J.N. Wang+, A.J. Schwartz+, T.G. Nieh+, C.T. Liu*, V.K. Sikka*, and D. Clemens**

+ Lawrence Livermore National Laboratory, Livermore, CA
* Martin Marietta Energy Systems, Inc., Oak Ridge, TN
** Pratt-Whitney, United Technologies, Jupiter, FL

Abstract

Creep of a TiAl alloy, having a composition of Ti-47Al-2Cr-2Nb (in atom %) and a fine-grained, fully-lamellar structure, was carried out at 760°C and stresses between 69–723 MPa. It was found that, in addition to having a good room temperature properties, the alloy exhibits higher creep resistance than other TiAl alloys with a similar composition. Both the creep data and microstructures of the alloy suggest that there exists a change in deformation mechanism from a glide-controlled process at high stresses to a recovery-controlled process at low stresses. Also, microstructural evidence indicates that the rate-controlling recovery mechanism is the climb of dislocation segments pinned by ledges at γ/α_2 interfacial boundaries.

Introduction

Current research efforts on γ-TiAl are primarily made to improve the room-temperature strength, toughness, and ductility, and to increase the high-temperature creep resistance. It is well known that the mechanical properties of γ-TiAl based two-phase alloys are strongly dependent upon microstructure [1]. By controlling thermomechanical processing, and subsequent heat treatment and cooling rate, three major types of microstructure can be produced: fully-lamellar, duplex, and equiaxed. The fully-lamellar structure consists of colonies of twin-related γ-TiAl lamellae interspersed with α_2-Ti_3Al laths. The duplex structure is composed of a mixture of equiaxed γ grains and fine lamellar grains, and the equiaxed structure is made up of equiaxed γ grains with α_2 particles at grain boundaries and triple junctions. The fully-lamellar structure has been found to have high creep strength but poor room-temperature ductility [2, 3], whereas the duplex microstructure gives high room-temperature ductility but poor high-temperature creep resistance (~two orders of magnitude lower than the fully-lamellar structure) [2]. In the fully-lamellar case, the mechanical properties are further dependent on the interlamellar spacing and the colony size in a polycrystal [1–6] and the lamellar orientation relative to the applied stress in a single crystal [7, 8].

Previously, γ-TiAl alloys were prepared mainly by casting methods. Only limited studies have been carried out on materials produced by powder metallurgy (PM) methods. The objective of this study is to report the high-temperature creep properties of a fully-lamellar TiAl alloy produced by a P/M technique. The room temperature as well as elevated temperature properties of the alloy were reported elsewhere [9].

Experimental

TiAl alloy used in this study was made by rapid solidification and powder extrusion. The as-extruded rods were stress relieved at 900°C in a vacuum of ~10^{-4} Pa for 2 h. Sheet specimens were fabricated from the annealed material by means of electrical discharge machining. They have a gage length of 25.4 mm, a thickness of 1.52 mm and a width of 5.08 mm. Creep experiments were conducted in a dead-load creep machine having a lever arm ratio of 16:1. Due to small strains (< 5%) involved, load was not reduced as strain accrued. Samples were tested in air in a split furnace with three zones. Temperature in each zone was controlled by individual thermocouples. The controlled temperature was within ±1°C of the required temperature along the whole gage length. Tests reported here were performed at a single temperature of 760°C and at a single stress or multiple stresses over a range of 69–723 MPa. Creep strains were measured using a dual dial gage average type extensometer having a strain resolution of 10^{-5}, and were recorded on a chart recorder.

Slices of the alloy were cut to 0.5 mm thickness followed by spark cutting of 3-mm discs. The discs were mechanically thinned to about 140 mm before electropolishing in a solution of 90% methanol, 9% sulfuric acid and 1% HF at 25V and 0°C. Conventional transmission electron microscopy and electron diffraction were performed on a JEOL 200CX microscope at. High resolution transmission electron microscopy was performed on a JEOL 4000EX system.

Results

Generally, the creep curve of TiAl exhibits three stages. After transient creep, a steady state was achieved in a single-stress test. As expected, the steady-state strain rate increases progressively with stress, which is shown in Fig. 1. If the creep strain rate $\dot{\varepsilon}$ is related to the stress σ by a power law: $\dot{\varepsilon} \sim \sigma^n$, where n is the stress exponent, then, n tends to decrease from > 7 in the high stress region to ~1.6 in the low stress region.

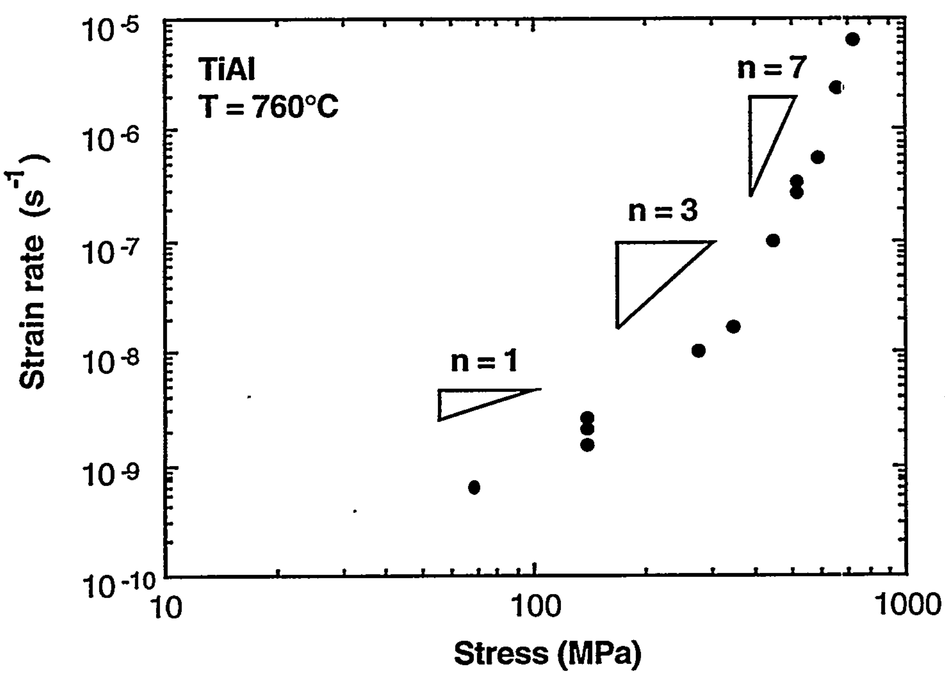

Fig. 1 Steady-state creep rate as a function of applied stress at 760°C.

To study the creep mechanism, stress reduction tests were performed. The transient creep behavior observed after a stress reduction apparently depends on the stress level before and after reduction. In the high-stress region (≥~ 400MPa), there is an immediate positive creep even after a stress reduction (e.g., 723 to 586 MPa in Fig. 2a). In contrast, in the low-stress region, when the stress is reduced from high to low stresses, in addition to the initial elastic contraction, there exists a period of negative creep, followed by an apparent zero creep (> 50 hours) and, then, an acceleration of creep (Fig. 2b) It is noted that the above transient creep behavior occurs at stress σ ~ 240 MPa.

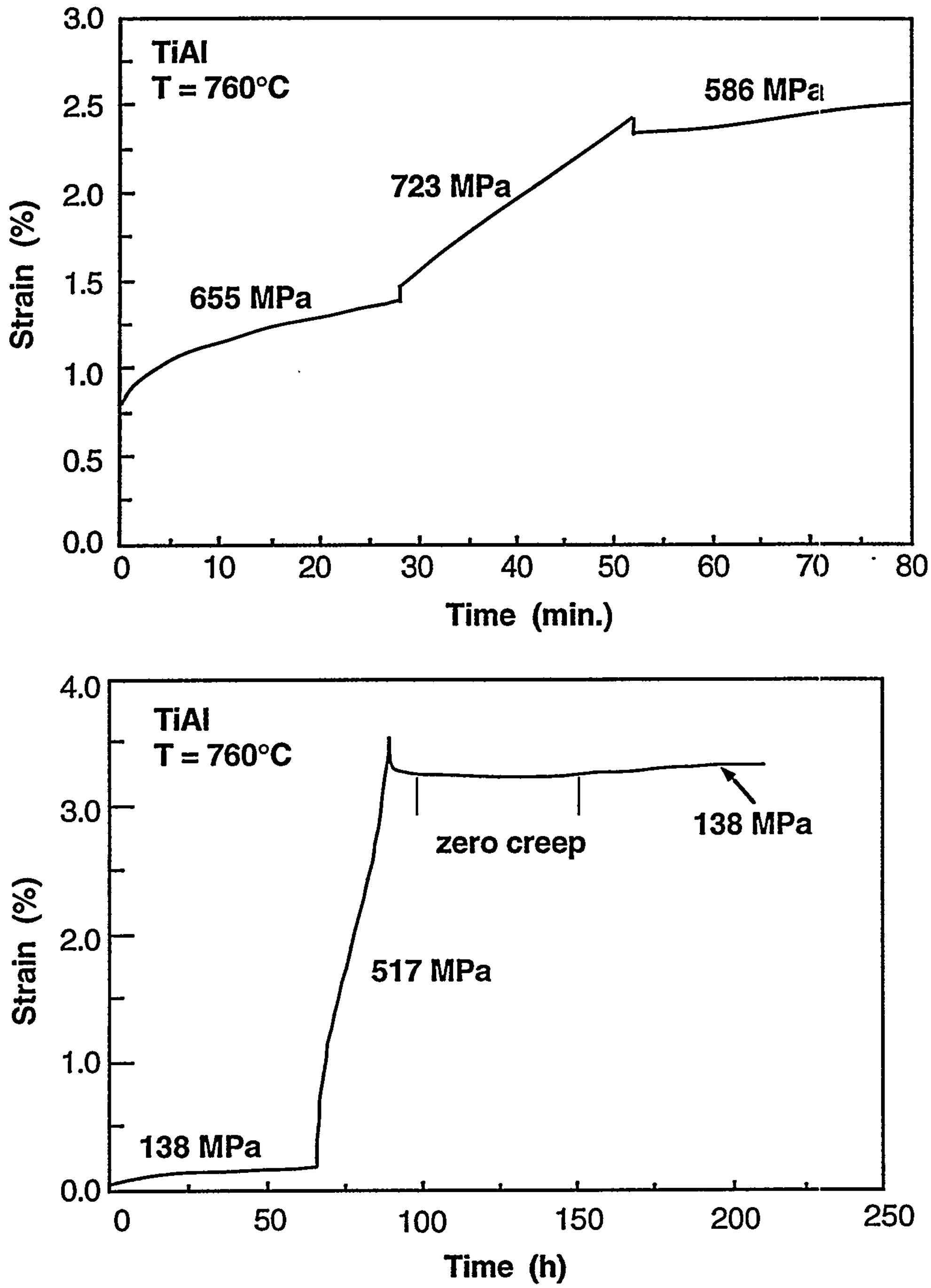

Fig. 2 Stress reduction tests in a) (top) the high-stress region, and b) (bottom) low-stress region.

The microstructure of the heat-treated sample exhibits a fully-lamellar structure with a colony size of ~65 μm and a nearly theoretical density. The lamellar grains consist of regular alternating γ and α_2 laths (Fig. 3a), which resulted from the solid state phase transformation of the primary disordered a dendrites [10]. The orientation relationship between γ and α_2 can be expressed as: $(111)_\gamma$ //$(0001)_{\alpha_2}$; $\langle 110\rangle_\gamma$ //$\langle 1120\rangle_{\alpha_2}$ which is consistent with previously results [11]. The α_2 platelets (20–76 nm wide) are long and straight, and quite regularly spaced between γ lamellae (~0.1–0.5 μm wide). The average interlamellar spacing is extremely fine (~0.1 μm). At many interfacial boundaries the γ/α_2 laths interlock with ledges as they meet (Fig. 3b). This irregular or serrated boundary inhibits interfacial sliding [12, 13]. Equiaxed γ grains of < 1 μm are occasionally observed along colony boundaries. Dislocations are rarely observed in both colony and γ grains.

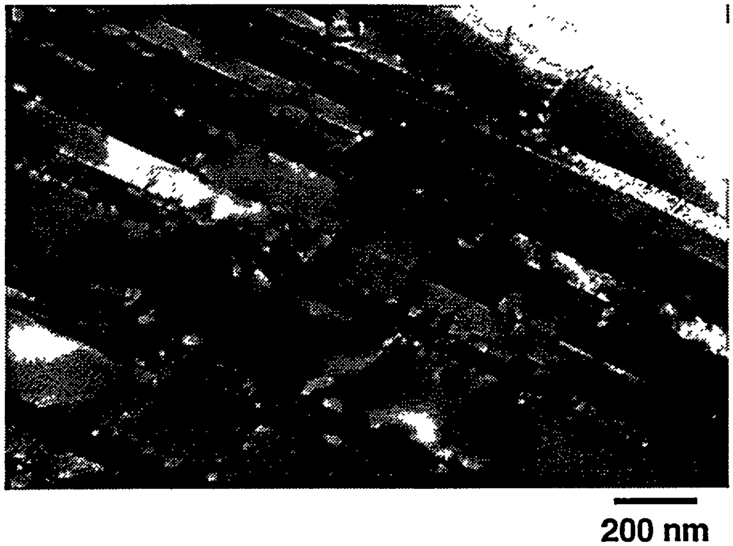

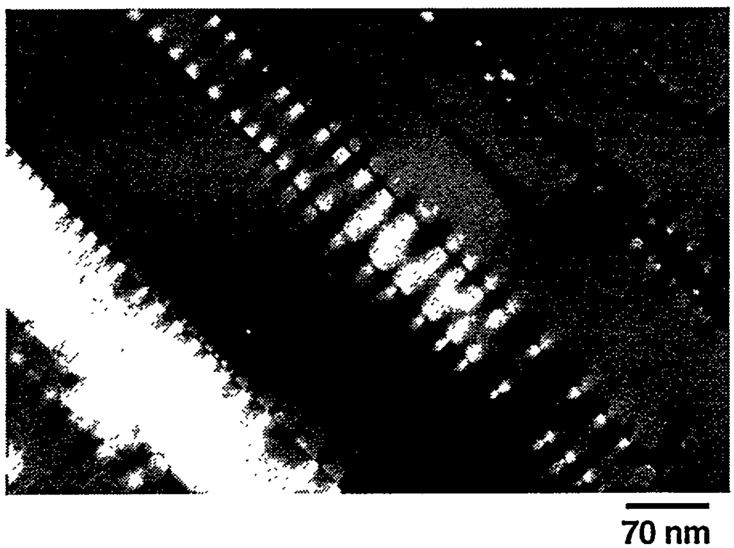

Fig. 3 $Ti_{49}Al_{47}Cr_2Nb_2$ alloy. (a) <110> zone axis bright-field image, and (b) <110> zone axis bright-field image.

Microstructures developed in samples crept to ~4% strain at high stresses (≥ 241 MPa) are inhomogeneous, varying from grain to grain and dependent upon their orientations relative to applied stress. Twins, tangled dislocations and long dislocation segments propagating across lamellar boundaries constitute the main feature of the microstructure of the γ lamellae (Fig. 4a). Also, twinning (i.e., probably the ordered (111)[112] type) occurs primarily across the lamellae, as shown in Ref. [11]. Although most twin boundaries show continuity across α_2 platelets, slight boundary offset is also observed (Fig. 4b), suggesting different shear deformation in adjacent γ lamellae as a result of twinning. Another structural feature is stacking faults. Partial dislocations are mainly located within interfacial boundaries. Randomly distributed dislocations spread within many γ lamellae. Tangling occurs mainly at the α_2/γ boundaries as well as twin boundaries. These observations indicate that deformation of both easy-type and hard-type had taken place [11].

Microstructures developed in samples creep deformed in the low-stress region (≤ 300 MPa) and low strains are significantly different from those seen in the high-stress samples. While secondary twins are well developed at high stresses, they are rarely observed in low-stress specimens. Also, although dislocation tangling and long dislocation segments propagating across lamellae are prominent features at high stresses, dislocations are only sporadically observed in low-stress specimens (Fig. 5). The observed dislocations are primarily within γ lamellae, and tend to be inclined at the same angle to the lamellar boundary.

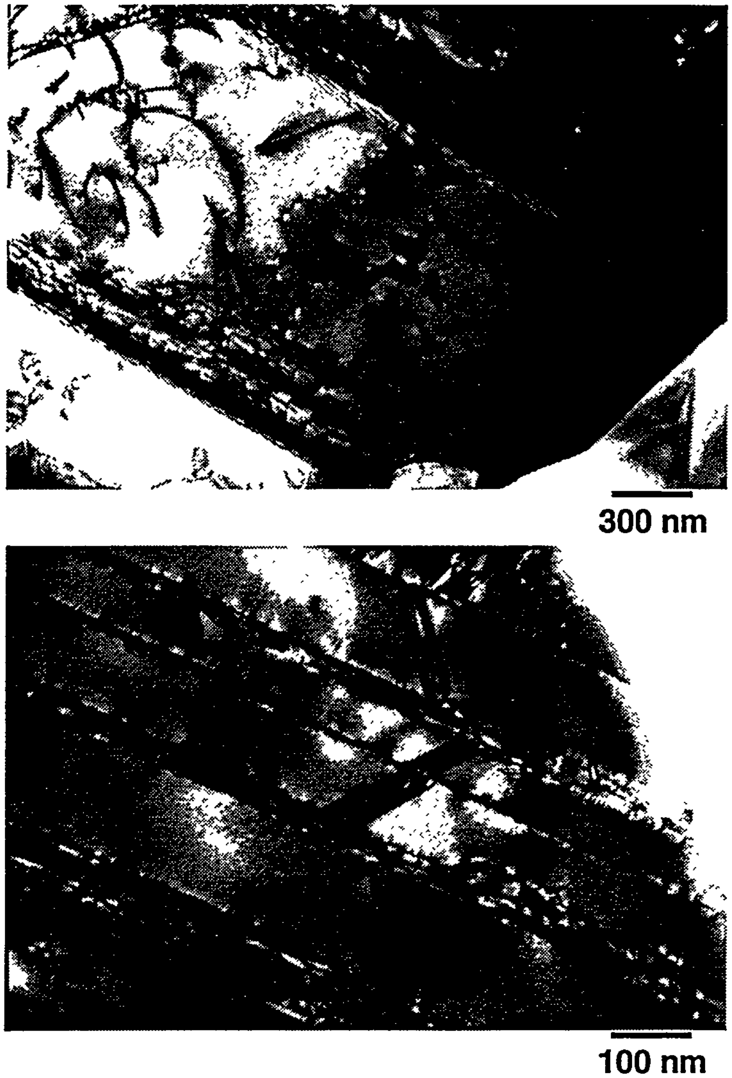

Fig. 4. Alloy crept at 760°C in the high-stress region (a) dislocation configuration and (b) twinning.

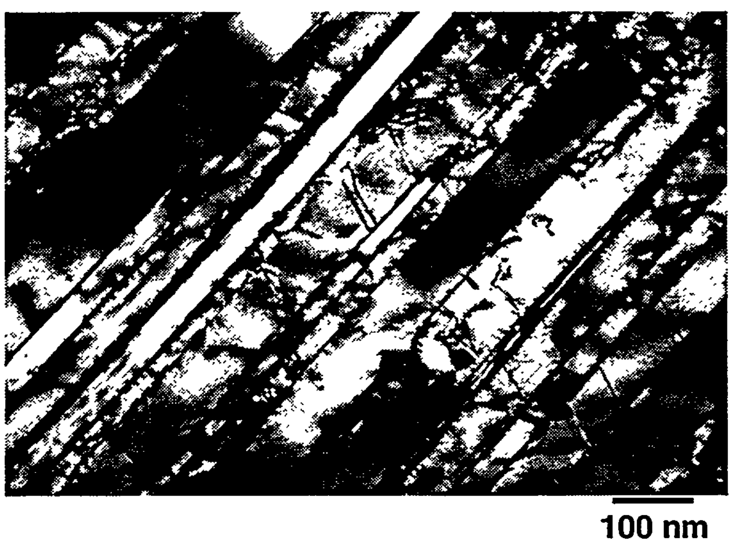

Fig. 5 Microstructure of sample crept at 760°C and 525 MPa.

In a specimen initially deformed at a high stress and, then, a lower stress, (e.g., in Fig. 3b), microstructure appears to be inhomogeneous, similar to those deformed at a single, high stress. Some grains show twins as well as a high density of free or tangled dislocations propagating across lamellar boundaries (Fig. 6). Since these microstructural features were not observed in specimen deformed at a single, low stress, they were probably generated when the specimen was deformed at the higher stress; the microstructure persists in the subsequent lower-stress deformation. In contrast, some grains may show only a few dislocations in γ lamellae, resulting probably from an unfavorable orientation for dislocation slip. Well defined subgrain boundaries are scarcely observed.

100 nm

Fig. 6 Microstructure of sample crept at 760°C, at an initial stress of 140 MPa, increased to 525 MPa and, then, reduced to the initial 140 MPa.

<u>Discussion</u>

A comparison of the creep resistance at 760°C among the presently-studied material and other TiAl alloys is given in Fig. 7 [14-24]. It is readily seen that the creep resistance of the present material is distinctively better than others. The improved creep property is believed to be resulted from the refined microstructure of the alloy.

It is known that mechanical properties of γ-TiAl with a fully-lamellar structure strongly depend on the interlamellar spacing, L [1–6]. This is because L determines the volume fraction of the hard-phase (i.e., α_2) which, in turn, determines the characteristic slip distance during dislocation-controlled creep. The maximum L value between the lamellae that are most favorably inclined for slip represents the minimum conditions for the onset of plastic deformation by dislocation slip [25].

The interlamellar spacing L in the present material is 0.1 µm [9]. This L is of several times smaller than those in typical cast alloys (e.g. L = 0.4–0.48 µm [26, 27]). Furthermore, the α_2 platelets in the present TiAl are long, straight, and quite regularly spaced within the fine lamellar structure, with the α_2 to γ lamella ratio close to 1:1. In contrast, the α_2 platelets in fine lamellar structures produced by fast cooling of cast TiAl contain many irregular and short segments [26]. Such microstructural imperfections reduce the load-bearing capability of the material. Therefore, the better creep resistance shown by the present alloy may be attributed to a combination of fine lamellar spacing and the unique morphology of the long, straight, and regularly-spaced α_2 platelets.

In the present study, twinning appears to have an insignificant contribution to the creep deformation of the alloy at low stresses (≤ 241 MPa). This is consistent with the previous observation that twinning is less important during high temperature deformation of lamellar TiAl [13]. Dislocations are observed within γ lamellae, and tend to be inclined at the same angle to the lamellar boundary. This observation is quite different from that on single crystals deformed at room temperature and at the same stress level [28]. In the latter case, many dislocations and twins are observed to run parallel to the lamellar boundaries (so called easy mode). Apparently, there is a change of dislocation slip from room to high temperatures. It is particularly pointed out that a thin layer of equiaxed γ grains (~1 µm) are present at colony boundaries. The role of these γ grains on the creep properties is unclear and needs further investigation.

The present experiments show that the deformation mechanism may be significantly different between high and low stresses, as evidenced by the facts that the stress exponent and microstructure change drastically from high to low stresses. Stress reduction tests show that creep at high stress may be glide-controlled as a positive creep rate is observed immediately after a stress reduction [29] (Fig. 2a). The observation of presence of dislocations both within and across γ lamellae supports such inference. If this is the case, then the high stress exponent and its decrease with stress is a result of control of dislocation glide whose velocity has an exponential dependence [30].

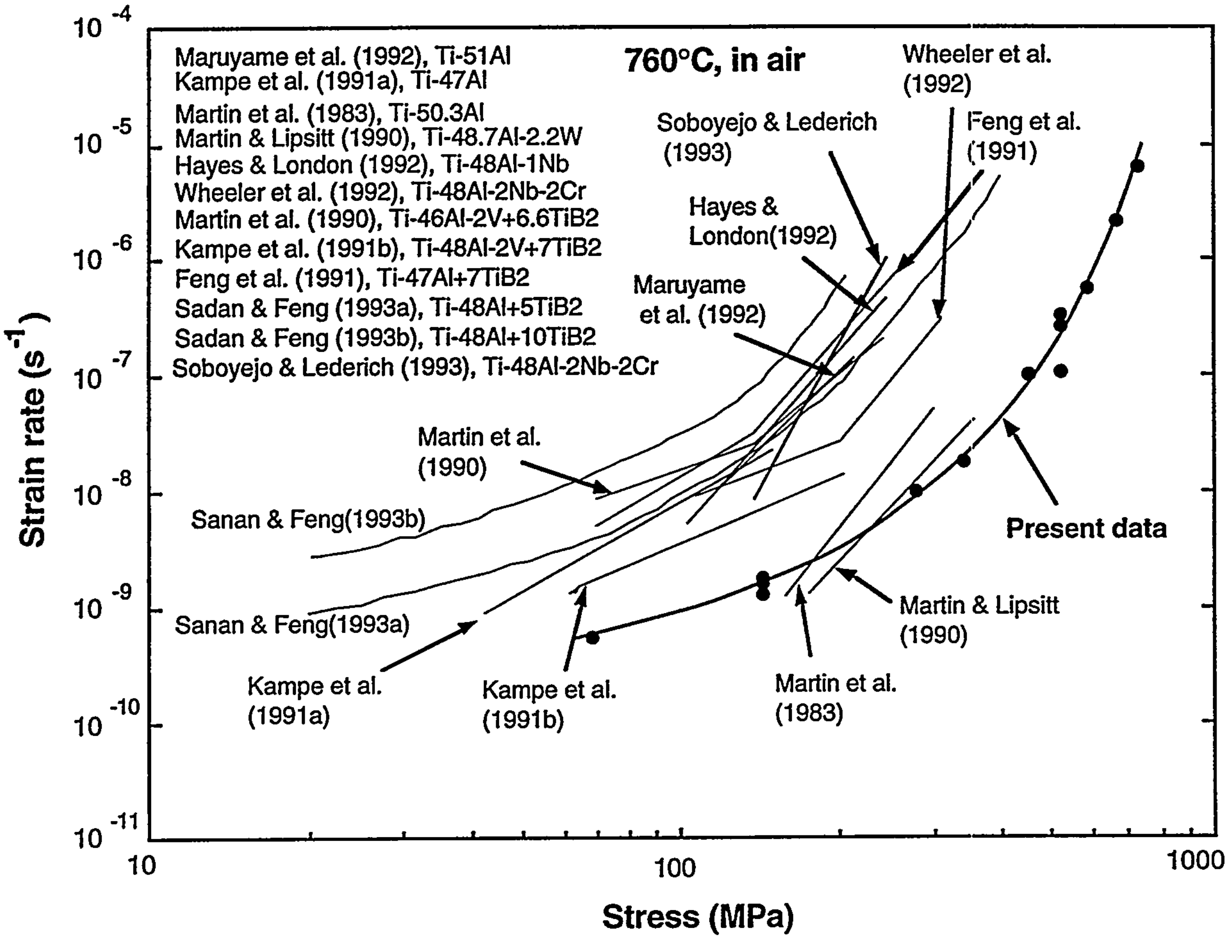

Fig. 7 A comparison of the creep resistance at 760°C among the presently-studied material and other TiAl alloys

In the low stress region (< 241 MPa), however, stress reduction tests show that, creep may be recovery-controlled as a zero creep is observed even after a small reduction [28]. Nevertheless, recovery processes such as dislocation climb and cross slip leading to curved dislocations and dislocation arrays or networks found in metals and disordered alloys were not observed in the present specimens. Instead, most dislocations are observed to intersect with α_2/γ boundaries. The possible recovery process is the climb of both ends of a dislocation line trapped in the boundaries (Fig. 5). It is known that the α_2/γ boundaries act as barriers to dislocation motion [31, 32]. In the case that a dislocation is pinned at the interfacial boundaries, the shear Orowan stress, τ_o, required to bow the dislocation out at the orientation parallel to the interfacial boundary is given by [25].

$$\tau_o = \frac{Gb}{2\pi L} \cdot \ln \frac{L}{2b}, \qquad (1)$$

where G is the shear modulus, b is the Burger's vector, and L is the width of γ lamellae. Taking G = 6 x 10^4 MPa for 760°C [31], b = 4 x 10^{-4} µm, and L = 0.3 µm, the average width of γ lamellae, τ_o is obtained to be 75.5 MPa. The present stress level at which recovery-controlled creep is observed is ≤ 137.8 MPa, which corresponds to a shear stress level of ≤ 79.6 MPa. This stress is close to the estimated Orowan stress (75.5 MPa). Thus, bowing of dislocations at the orientation parallel to the interfacial boundary may be impossible under the condition of $\sigma \leq 137.8$ MPa in the present alloy. It may be concluded,that in order for dislocation motion to proceed, climb of the segments trapped in the boundary must take place.

It is interesting to note that n = ~1.6 at low stress. Deformation studies on a near γ Ti-Al+W with a lamellar structure showed that the strain rate was independent of the colony grain size at 760°C and 276 MPa [33]. Thus, the low n behavior may be induced by an intragranular process. This is possible because creep strains achieved at low stress are very low (< 0.5%) and a true steady state microstructure might not be achieved; deformation may take place at a dislocation density or at a dislocation structure insensitive to the applied low stress.

Conclusion

The presently-studied TiAl alloy with a fine, fully-lamellar structure shows a better creep resistance than those previously reported for other TiAl alloys. This improved property is attributed to the combined effects of the fine lamellar structure and the unique, regular morphology of the α_2 platelets interspersed between γ lamellae. Creep data and microstructural characteristics suggest that deformation of the present alloy at 760°C may be glide-controlled at high stresses (≥ 241 MPa) but recovery-controlled at low stresses (≤ 241 MPa). Creep at low stresses is insensitive to dislocation structure, and the rate is controlled by the climb of dislocation segments trapped in α_2/γ interfacial boundaries.

Acknowledgments

This work was partly performed under the auspices of the U.S. Department of Energy through contract No. W-7405-Eng-48 with Lawrence Livermore National Laboratory and contract No. DE-AC-05-84OR21400 with Martin Marietta Energy System, Inc, and, partially supported by the Pratt-Whitney, United Technologies, Independent Research and Development Program.

References

1. Y.-W. Kim, Acta Metall. Mater., **40**, 1121 (1992).
2. D.S. Shih, S.-C. Huang, G.K. Scarr, H. Jang and J.C. Chesnutt, in "Microstructure-Property Relationships in Titanium Aluminides and Alloys", eds. Y. W. Kim and R. Boyer, The Minerals, Metals & Materials Society, Warrendale, PA, p. 135 (1991).
3. S. Mitao, S. Tsuyama and K. Minakawa, in "Microstructure/Property Relationships in Titanium Aluminides and Alloys", eds. Y. W. Kim and R. Boyer, The Minerals, Metals & Materials Society, Warrendale, PA, p. 297 (1991).
4. Y.-W. Kim, J. Metals, **46**, 30 (1994).
5. M. Yamaguchi and H. Inui, in "Structural Intermetallics", eds. R. Darolia, J.J. Lewandowski, C.T. Liu, P.L. Martin, D.B. Miracle, and M. Nathal,TMS, Warrendale, PA, p. 127 (1993).
6. S.C. Huang, in "Structural Intermetallics", eds. R. Darolia, J.J. Lewandowski, C.T. Liu, P. L. Martin, D.B. Miracle, and M. Nathal,TMS, Warrendale, PA, p. 299 (1993).
7. T. Fujiwara, A. Nakamura, H. Hosomi, S. R. Nishitani, Y. Shirai and M. Yamaguchi, Philos. Mag. A, **61**, 591 (1990).
8. S. R. Nishitani, M. H. Oh, A. Nakamura, T. Fujiwara and M. Yamaguchi, J. Mater. Res., **5**, 484 (1990).
9. C.T. Liu, P.J. Maziasz, D.R. Clemens, J.H. Schneibel, V.K. Sikka, T.G. Nieh, J. Wright, and L. R. Walker, in this proceeding.
10. P.A. Beaven, F. Appel, B. Dogan and R. Wagner, in "Ordered Intermetallics– Physical Metallurgy and Mechanical Behavior", eds. C.T. Liu, G. Sauthoff and R.W. Cahn, Kluwer Academic Publishers, p. 413 (1992).
11. H. Inui, M.H. Oh, A. Nakamura and M. Yamaguchi, Philos. Mag. A, **66**, 539 (1992).
12. R. W. Hayes and B. London, Acta Metall. Mater., **40**, 2167 (1992).
13. M. Es-Souni, A. Bartels and R. Wagner, Acta Metall. Mater., **43**, 153 (1995).
14. K. Maruyama, T. Takahashi and H. Oikawa, Mater. Sci. Engng., **A153**, 433 (1992).
15. S. L. Kampe, L. Christodoulou and J. A. Clark, TMS symposium on Creep and Fatique of Metal Matrix Composites, New Orleans, LO (1991a).
16. S.L. Kampe, J.D. Bryant and L. Christodolou, Metall. Trans., **22A**, 447 (1991b).

17. P.L. Martin, M.G. Mendiratta and H.A. Lipsitt, Metall. Trnas., **14A**, 2170 (1983).
18. P.L. Martin and H.A. Lipsitt, in B.L. Wilshire and R. W. Evans (eds.), Proc. 4th Int. Conf. on Creep and Fracture of Engineering Materials and Structures, Institute of Metals, London, p. 225 (1990).
19. D.A. Wheeler, B. London and D.E. Larson, Jr., Scripta Metall. Mater., **26**, 939 (1992).
20. P.L. Martin, D.H. Carter, R.M. Aikin, Sr., R.M. Aikin, Jr., and L. Christodoulou, in "Proc. 4th Int. Conf. on Creep and Fracture of Engineering Materials and Structures", eds. B.L. Wilshire and R.W. Evans, Institute of Metals, London, p. 265 (1990).
21. C.R. Feng, H.H. Smith, D.J. Michel and C.R. Crowe, in "Microstructure/Property Relationships in Titanium Aluminides and Alloys", eds. Y. W. Kim and R. Boyer, The Metallurgical Society of AIME, Warrendale, PA, p. 353 (1991).
22. K. Sadananda, C.R. Feng, H.N. Jones and J.J. Petrovic, in "Structural Intermetallics", eds. R. Darolia, J.J. Lewandowski, C.T. Liu, P.L. Martin, D.B. Miracle, and M. Nathal,TMS, Warrendale, PA (1993).
23. W.O. Soboyejo and R.J. Lederich, in "Structural Intermetallics", eds. R. Darolia, J.J. Lewandowski, C.T. Liu, P.L. Martin, D.B. Miracle, and M. Nathal,TMS, Warrendale, PA, p. 353 (1993).
24. M. Takeyama, T. Kumagai, M. Nakamura and M. Kikuchi, in "Structural Intermetallics", eds. R. Darolia, J. J. Lewandowski, C. T. Liu, P. L. Martin, D. B. Miracle, and M. Nathal,TMS, Warrendale, PA, p. 167 (1993).
25. J.P. Hirth and J. Lothe, "Theory of Dislocations", Wiley, New York (1982).
26. Y.-W. Kim, Mater. Sci. Engng., (in press) (1995).
27. R.V. Ramanujan, P.J. Maziasz, and C.T. Liu, submitted to Acta Metall. (1995).
28. M. Es-Souni, A. Bartels and R. Wagner, Mater. Sci. Engng., **A171**, 127 (1993).
29. W.J. Evan and B. Wilshire, "Creep of Metals and Alloys", The Institute of Metals, London (1985).
30. J. Cadek, "Creep in Metallic Materials", Elsevier, Amsterdam (1988).
31. H.A. Lipsitt, D. Shechtman and R. E. Schafrik, Metall. Trans., **6A**, 1991 (1975).
32. S. Mitao, S. Tsuyana and K. Minakawa, in "Structural Intermetallics", eds. R. Darolia, J.J. Lewandowski, C.T. Liu, P.L. Martin, D.B. Miracle, and M. Nathal,TMS, Warrendale, PA, p. 297 (1993).
33. J. Triantafillou, J. Beddoes, L. Zhao and W. Wallace, Scripta. Metall. Mater., **31**, 1365 (1994).